

## Deformation of the Free Surface in a Moving Locally-Heated Thin Liquid Layer

O. A. Kabov, J. K. Legros, I. V. Marchuk, and B. Sheid

Received May 23, 2000

**Abstract**— Liquid film flow on a vertical surface is studied experimentally and theoretically under the determining influence of the thermocapillary forces. In the two-dimensional steady-state case the shape of the film surface is calculated numerically within the thin layer approximation with allowance for the temperature dependence of the viscosity of the liquid and redistribution of the heat flux in the heating element. A local heat source was used in the experiments to produce temperature gradients up to 10 K/mm on the liquid surface. The film thickness was determined by means of the schlieren method with reflection. The relative thickness of the roller in the upper heater edge zone, characteristic of the formation of regular structures, is measured. The thickness is  $h/h_0 = 1.32 \pm 0.07$ , which agrees satisfactorily with the results of numerical calculations.

Thin liquid films falling under the action of gravity are a very simple but fairly common case of multi-phase flow of a nonisothermal medium with a deformable liquid-gas interface. In this flow the surface forces can predominate over the body forces or be comparable with them.

In [1–3] experimental procedures were developed for the previously uninvestigated range of regime parameters at low Reynolds numbers (film thickness of 40–100  $\mu\text{m}$ ) and high temperature gradients on the phase interface (up to 10–15 K/mm). The phenomenon of formation of a three-dimensional self-organizing structure in a thin liquid film falling under the action of gravity when the film is locally heated by the base plate was detected and investigated. In Fig. 1 we have reproduced schlieren photos of the regular structures.

For a certain threshold heat flux density  $q_r$  on the heater the flow breaks down into vertical streamlets spaced at a certain wavelength  $\Lambda$  with a thin film between them. A much smaller vertical streamlet is formed in the central part of each horseshoe-shaped structure. The onset of a horizontal liquid roller in the upper heater edge zone, simultaneously with the formation of the structures, is common to all the experiments. This phenomenon was reproduced for various regime parameters and heater dimensions. By means of direct measurements of the temperature field on the liquid film surface using infrared thermography it was established that the formation of the structures is thermocapillary in nature. A region with maximum surface temperature gradient duplicating the shape of the structures develops in the horizontal roller zone [1, 3]. In the above studies the film thickness was not measured.

The deformations of the free surface of thin liquid layers, including traveling layers, were simulated in [4, 5] using an evolution equation for the film thickness of the Benet equation type obtained in the longwave approximation. The possible mechanism of rivulet formation in a falling film described in [5] is thermocapillary and determined by the intensity of heat transfer between the liquid and gas phases. It was assumed that the substrate temperature is constant. The evolution of the surface shape was calculated for the Biot number  $Bi = 1$ . For the process studied in this paper the condition  $Bi = 1$  corresponds to a heat transfer rate on the film surface  $(5\text{--}10) \cdot 10^3 \text{ W}/(\text{m}^2 \cdot \text{K})$ , which is greater than the heat transfer coefficient observed in practice by 2–3 orders. In [5] this value of  $Bi$  seems to have been chosen because in the case of  $Bi = 1$  the linear theory gives the maximum thermocapillary instability. An analysis of the experimental studies [1–3] shows that the heat transfer on the liquid-gas interface only slightly affects the instability wavelength  $\Lambda$  and the formation of the regular structures detected under local heating.

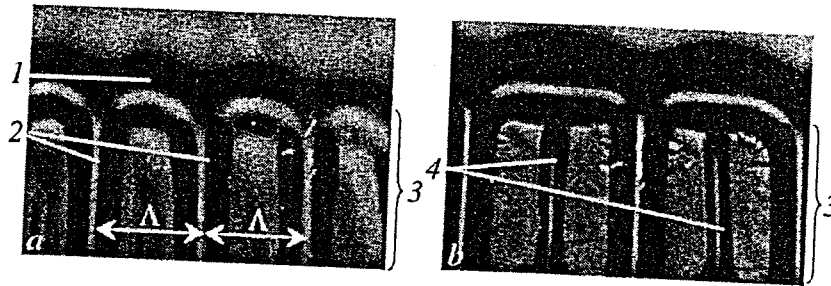


Fig. 1. Regular structures on the surface of a locally heated falling liquid film for  $C = 25\%$ ,  $T_0 = 20^\circ\text{C}$ , and  $\text{Re} = 1$ :  $q = q_r = 2.4 \text{ W/cm}^2$  (a) and  $q = 4.2 \text{ W/cm}^2$  (b). Roller (1), streamlet (2), heater (3), and central streamlet (4)

In [3] the thermocapillary deformation initiated by local heating of the film was calculated for the wall conditions  $T = \text{const}$  and  $q = \text{const}$ . In [6] the shape of the film surface was calculated on the basis of the temperature distribution over the film surface measured by means of infrared thermography. It was shown that the temperature gradients on the film surface measured under local heating may lead to the onset of a thermocapillary reverse flow counter to the main flow. In the above studies only two-dimensional models of the locally heated film were considered; therefore, the question of simulating the wavelength of the regular structures remains open. In [3, 6] the temperature dependence of the viscosity was neglected.

The aim of the present paper is to obtain the basic governing laws of film flow under the action of gravity and local heating up to the formation of regular structures. The numerical calculations take into account the temperature dependence of the liquid viscosity and the heat flux redistribution in the heating element. The angle of inclination of the interface was measured experimentally using the schlieren method with reflection. Experimental data concerning the film thickness profile in the heating-element zone are obtained for various Reynolds numbers and heat flux densities.

## 1. FORMULATION OF THE PROBLEM AND METHOD OF SOLUTION

Let a thin film flow along the  $x$  axis down a flat substrate with a local heat source inclined at an angle  $\Theta$  to the horizontal (Fig. 2). Local heating means that the heat flux density on the substrate is a finite function of the variable  $x$ . The surface tension and the viscosity are assumed to depend on the temperature

$$\sigma = \sigma_0 + \sigma_T(T - T_0), \quad \mu = \mu(T) > \mu_m > 0 \quad (1.1)$$

After a scales analysis, in the thin layer approximation the equations of steady-state plane motion of a liquid film with a free surface take the form:

$$0 = \sigma_0 h_{xxx} - \rho g \cos \Theta h_x + \rho g \sin \Theta + (\mu(x, y) u_y)_y \quad (1.2)$$

$$u_x + v_y = 0 \quad (1.3)$$

$$u T_x + v T_y = a T_{yy} \quad (1.4)$$

The boundary conditions have the following form: the no-slip condition

$$u(x, 0) = v(x, 0) = 0 \quad (1.5)$$

thermocapillary effect on the film surface

$$[\mu u_y](x, h(x)) = \sigma_T T_S(x) \quad (1.6)$$

a given constant specific liquid flow rate

$$\int_0^{h(x)} \rho u(x, y) dy = \Gamma \quad (1.7)$$

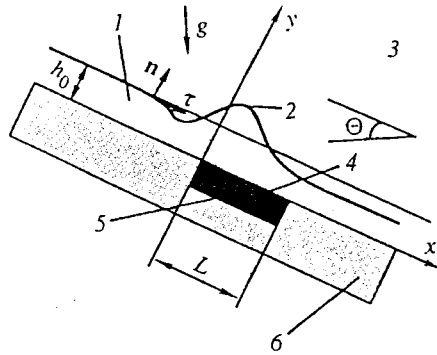


Fig. 2. Film flow diagram. Liquid (1), roller (2), gas (3), cover plate (4), heater (5), and thermal insulation (6)

a given initial temperature of the falling isothermal film

$$T(-\infty, y) = T_0$$

no heat transfer on the free surface

$$T_y(x, h(x)) = 0$$

a local heat source on the interval  $[0, L]$

$$-\lambda T_y(x, 0) = q(x)(\chi(x) - \chi(x - L))$$

Here,  $u$  and  $v$  are the longitudinal and transverse velocity components,  $T$  is the temperature,  $T_0$  is the initial temperature of the film,  $T_S(x) = T(x, h(x))$  is the surface temperature,  $h(x)$  is the film thickness,  $\Gamma$  is the specific flow rate,  $q(x)$  is the heat flux density distribution over the local heat source,  $L$  is the length of the heating element,  $\lambda$  is the thermal conductivity of the liquid, and  $\chi$  is the Heaviside step function.

Integration of Eq. (1.2) with allowance for the boundary conditions (1.5), (1.6) gives the expression for the velocity

$$u(x, y) = -(\sigma_0 h_{xxx} - \rho g \cos \Theta h_x + \rho g \sin \Theta) \int_0^y \frac{\zeta - h(x)}{\mu(x, \zeta)} d\zeta + \sigma_T T_S(x) \int_0^y \frac{d\zeta}{\mu(x, \zeta)} \quad (1.8)$$

After substitution of expression (1.8) in the balance relation (1.7) for the flow rate, the latter takes the form:

$$(\sigma_0 h_{xxx} - \rho g \cos \Theta h_x + \rho g \sin \Theta) \int_0^{h(x)} \int_0^y \frac{\zeta - h(x)}{\mu(x, \zeta)} d\zeta dy + \sigma_T T_S(x) \int_0^{h(x)} \int_0^y \frac{d\zeta dy}{\mu(x, \zeta)} = \frac{\Gamma}{\rho} \quad (1.9)$$

Integrating by parts, we transform the double integrals and write the film thickness equation in the form:

$$(\sigma_0 h_{xxx} - \rho g \cos \Theta h_x + \rho g \sin \Theta) \int_0^{h(x)} \frac{(h(x) - y)^2}{\mu(x, y)} dy + \sigma_T T_S(x) \int_0^{h(x)} \frac{h(x) - y}{\mu(x, y)} dy = \frac{\Gamma}{\rho} \quad (1.10)$$

If in Eq. (1.10) we neglect the capillary and hydrostatic pressures (the first and second terms of the expression in parentheses), then, using the initial film thickness  $h_0$  as the length scale, we can reduce equation (1.10) to the simple dimensionless form:

$$H^3 - \frac{3\mu_2}{2\mu_1} K_T H^2 - \mu_2 = 0 \quad (1.11)$$

$$H = h/h_0, \quad \mu_0 = \mu(T_0), \quad K_T(x) = -\sigma_T T_S(x) / (\rho g h_0 \sin \Theta)$$

Here,  $K_T(x)$  is the ratio of the thermocapillary tangential stress to the tangential stress on the wall in the absence of temperature effects determined by dependences (1.1). The parameters

$$\mu_1(x) = h^2(x) \left[ 2\mu_0 \int_0^{h(x)} \frac{h(x) - \zeta}{\mu(x, \zeta)} d\zeta \right]^{-1}, \quad \mu_2(x) = h^3(x) \left[ 3\mu_0 \int_0^{h(x)} \frac{(h(x) - \zeta)^2}{\mu(x, \zeta)} d\zeta \right]^{-1}$$

are the effective dimensionless viscosity coefficients. The expressions for the parameters  $\mu_1$  and  $\mu_2$  reflect the fact that the friction force in the film decreases with increase in the distance from the wall. The value of  $\mu_1$  is determined by the variation of the viscosity across the film with a weight inversely proportional to the distance from the wall. The value of  $\mu_2$  is determined by the variation of the viscosity across the film with a weight inversely proportional to the square of the distance from the wall. If the viscosity is independent of the temperature, then  $\mu_1 = \mu_2 = 1$ . From Eq. (1.11) it follows that in the absence of a thermocapillary effect the second term on the left side of the equation vanishes and the dimensionless film thickness is determined only by the parameter  $\mu_2$ :  $H = \mu_2^{1/3}$ .

A correction for the temperature dependence of the viscosity is usually made using  $\mu_F = \mu(T_F)$  as the effective viscosity [7], where  $T_F$  is the weighted-mean film temperature. In the neighborhood of the heater surface the liquid can have a temperature much higher than the weighted-mean film temperature and, as a result, a lower viscosity. The film, as it were, slips over the heater and its thickness decreases significantly. In this case the change in thickness will be greater than that given by the correction for  $T_F$ .

The characteristic dimensions of the strains on the film surface are comparable with the capillary length  $l_\sigma = \sqrt{\sigma_0/(\rho g)}$ ; therefore, we cannot neglect the capillary pressure. In this case there is a natural length scale  $l_\sigma$  and equation (1.10) can conveniently be written in the dimensionless variables  $X_\sigma = x/l_\sigma$ ,  $\delta = h/l_\sigma$ ,  $\theta = (T - T_0)/\Delta T$ ,  $Y_\sigma = y/l_\sigma$ :

$$\delta''' - \cos \Theta \delta' + \sin \Theta - \frac{\delta_0^3 \mu_2 \sin \Theta}{\delta^3} - \frac{3Cr\theta'_s \mu_2}{2\mu_1 \delta} = 0 \quad (1.12)$$

$$Cr = \frac{\delta_T \Delta T}{\delta_0}, \quad \Delta T = [c_p \Gamma]^{-1} \int_0^L q(x) dx$$

Here,  $Cr$  is the deformability criterion,  $\theta_s = \theta(X_\sigma, \delta(X_\sigma))$  is the surface temperature,  $\Delta T$  is the characteristic temperature difference in the film, and  $c_p$  is the specific heat of the liquid. At small angles  $\Theta$  the weight of the hydrostatic pressure term in (1.10) becomes significant and this term also cannot be omitted.

We introduce the dimensionless velocities  $U = u/u_0$  and  $V = v/v_0$ , where  $u_0 = \rho g \sin \Theta h_0^2/\mu$ ,  $v_0 = \varepsilon u_0$ , and  $\varepsilon = h_0/L$ . From Eqs. (1.8), (1.10) there follows the expression for the velocity  $U$

$$U = \left[ -\frac{3\mu_2}{2\mu_1 H} K_T - \frac{\mu_2}{H^3} \right] \int_0^Y \frac{\zeta}{\mu_3} d\zeta + \left[ \frac{\mu_2}{H^2} + \left( \frac{3\mu_2}{2\mu_1} - 1 \right) K_T \right] \int_0^Y \frac{1}{\mu_3} d\zeta \quad (1.13)$$

where  $H = h/h_0$ ,  $\mu_3 = \mu(x, y)$ ,  $Y = y/h_0$ , and  $X = x/L$  are the dimensionless film thickness, viscosity, and coordinates, respectively. In the absence of temperature factors expression (1.13) gives a velocity distribution that coincides with the semiparabolic velocity profile obtained by Nusselt. From expression (1.13) and the continuity equation (1.3) there follows the expression for the transverse velocity component

$$V = -\frac{\partial}{\partial X} \left( \left[ -\frac{3\mu_2}{2\mu_1 H} K_T - \frac{\mu_2}{H^3} \right] \int_0^Y \frac{Y\zeta - \zeta^2}{\mu_3} d\zeta + \left[ \frac{\mu_2}{H^2} + \left( \frac{3\mu_2}{2\mu_1} - 1 \right) K_T \right] \int_0^Y \frac{Y - \zeta}{\mu_3} d\zeta \right) \quad (1.14)$$

The change of variable  $\eta = y/h(x)$  straightens the free boundary of the film. In dimensionless variables the heat conduction equation (1.4) has the form:

$$3Pe\varepsilon(H^2 U \theta_X + (V - YH_X U)H\theta_\eta) = \theta_{\eta\eta} \quad (1.15)$$

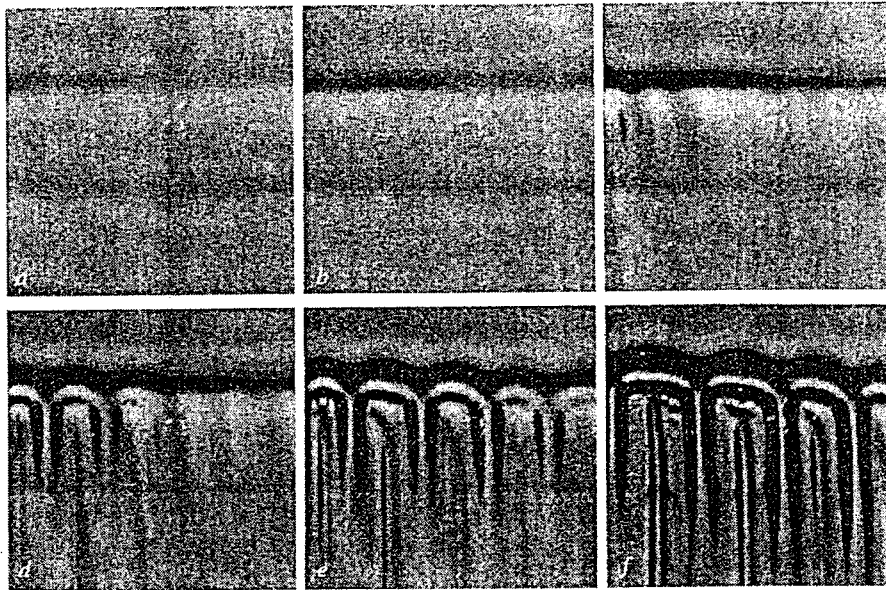


Fig. 3. Dynamics of the formation of regular structures under local heating of a falling liquid film for  $C = 25\%$ ,  $T_0 = 20^\circ\text{C}$ ,  $\text{Re} = 0.5$ ,  $h_0 = 0.10$  mm, and  $l_\sigma = 1.94$  mm:  $q = 0.3$  W/cm<sup>2</sup> (a),  $q = 0.63$  (b),  $q = 1.12$  (c),  $q = 1.21$  (d),  $q = 1.5$  (e), and  $q = 2.11$  W/cm<sup>2</sup> (f)

where  $\text{Pe} = \text{RePr} = c_p \Gamma / \lambda$  is the Péclet number.

Equation (1.15) was solved numerically using a downstream explicit scheme of the relaxation method. The flow parameters were renewed each  $N$  iterations ( $N$  is the number of grid points in the variable  $X$ ). The film thickness  $H$  and the velocities  $U$  and  $V$  were calculated. The nonlinear equation (1.12) was solved numerically by minimization of the residual functional using the conjugate gradient method. We used the quantities  $\theta'_s$  and  $\mu(x, y)$  calculated from the film temperature known from the previous time step of the relaxation method. As the initial approximation of the film thickness, we took the solution of Eq. (1.11). The velocities  $U$  and  $V$  were calculated from formulas (1.13) and (1.14). The criterion for the termination of the iteration process was the condition that the norm of the residual vector of the finite-difference analog of Eq. (1.15) be less than a given accuracy after the next flow recalculation. The numerical calculations of Eq. (1.15), carried out without temperature factors for the boundary conditions  $q = \text{const}$  and  $T = \text{const}$  on the heater surface, were compared with the solutions obtained in [7]. For the linearized equation (1.12) in the case of constant viscosity the fundamental solutions [6] were found. These solutions were used to test the algorithm for the numerical solution of Eq. (1.12).

## 2. EXPERIMENTAL SETUP

Under the action of gravity a liquid film flowed out from a plane slit 0.25 mm high and 210 mm wide formed by the base plate and a stainless-steel plate 35 mm long. The base plate was made from a 240 × 250 mm textolite block 30 mm thick. The heater was a film resistor in a ceramic shell 0.8 mm thick soldered to a stainless-steel cover plate 2.28 mm thick (Fig. 2). The heater length and width (across the flow) were  $L = 6.7$  mm and 68 mm, respectively. The cavity around the heater all entire the film flow region were covered by a mixture of epoxy resin and charcoal with a thermal conductivity 100 times lower than that of the stainless-steel. The entire surface over which the film flowed was polished.

The distance from the nozzle to the heat source (38.2 mm) was chosen so that, on the one hand, the film flowed onto the heater with a stabilized velocity profile and thickness and, on the other hand, the heating element was located in the region of the smooth waveless part of the film. The film, an aqueous solution of ethyl alcohol (mass concentration  $C = 10$  and 25%) had the initial temperature  $T_0 = 20^\circ\text{C}$ . The flow took place in air under steady-state conditions. The liquid was significantly underheated with respect to the

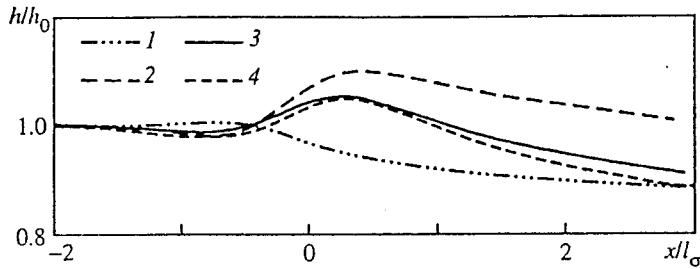


Fig. 4. Relative film thickening along a plate with a local heat source. Curve 1 corresponds to the calculation made with allowance for only the temperature dependence of the viscosity ( $\sigma_T = 0$ ), curve 2 to the calculation made with allowance for only the thermocapillary effect ( $\mu = \mu_0 = \text{const}$ ), curve 3 to the calculation made with allowance for both effects, and curve 4 to the schlieren measurements.  $C = 25\%$ ,  $T_0 = 20^\circ\text{C}$ ,  $\text{Re} = 1$ ,  $q = 1.38 \text{ W/cm}^2$ ,  $h_0 = 0.126 \text{ mm}$ , and  $l_\sigma = 1.94 \text{ mm}$

boiling point at atmospheric pressure. In the neighborhood of the film the air temperature was maintained equal to the initial film temperature within  $\pm 1^\circ\text{C}$ . The Re number ( $\text{Re} = \Gamma/\mu$ ) varied on the interval from 0.09 to 2.

The average heat flux density  $q$  was determined on the basis of the power released at the heater and varied from 0.2 to  $7 \text{ W/cm}^2$ . The angle of inclination of the gas-liquid interface was measured by means of the modified schlieren method. The film was illuminated by nine plane incoherent collimated light beams of various intensity. The central beam was incident along the normal to the base plate. The other light beams fell on the film at certain angles. The measurement field on the film was a  $27.9 \times 19.9 \text{ mm}$  region in which the beams intersected. The radiation reflected from the film was directed by a semitransparent mirror through a slit onto a video receiver. For a smooth film the video receiver was illuminated only by the central beam. In the case of a deformed film the video lens was struck by radiation falling on the given section of the film in a near-normal direction. The optical system had an error of not more than  $1'$  and made it possible to carry out measurements on the range of angles of inclination of the film  $\pm 1.7^\circ$ . The film thickness was determined by the numerical integration method using the initial calculated thickness  $h_0 = (v^2/g \sin \Theta)^{1/3} (3\text{Re})^{1/3}$ . For a the film strain amplitude of the order of  $50 \mu\text{m}$  the measurement error was not greater than  $0.5 \mu\text{m}$ .

### 3. DISCUSSION OF THE EXPERIMENTAL RESULTS AND THE CALCULATIONS

In Fig. 3 we have reproduced some schlieren images of the film for various heat fluxes at  $\text{Re} = 0.5$ . These make it possible to trace the dynamics of formation of the regular structures. The initial thickness of the falling liquid layer  $h_0 = 100 \mu\text{m}$ . Local heating of the film leads to the onset of steady-state horizontal film thickening — a roller at the upper edge of the heating element. The roller, formed by a surface force of a thermocapillary nature, developed at the smallest heat fluxes. For  $q = 0.3 \text{ W/cm}^2$  and  $0.63 \text{ W/cm}^2$  the maximum relative thickening in the roller  $h_{mR}/h_0 = 1.06$  and  $1.16$ , respectively. Both regimes are steady-state. The film remains smooth ahead of the roller and in the middle of the heater.

When  $q \geq 1.1 \text{ W/cm}^2$  the roller loses stability and vertical strains develop in the film. With increase in the heat flux ( $q = 1.2 \text{ W/cm}^2$ ) instability develops in the direction across the film flow, the strain amplitude increases, and horseshoe-shaped structures begin to develop. When  $q = q_r = 1.5 \text{ W/cm}^2$  a chain of structures is formed along the entire heater. The roller grows significantly larger and its maximum relative thickening  $h_{mR}/h_0 = 1.3$ . With further increase in the heat flux density the number of structures spread over the heater decreases. For  $q \geq 1.1 \text{ W/cm}^2$  the regimes are quasi-steady. With variation of the heat flux density the streamlets were able to travel across the heater or oscillate about a certain centre of equilibrium.

The photos reproduced in Fig. 1 show the dynamics of development of the structures at  $\text{Re} = 1$ . These photos and those in Fig. 3 have the same scale and, moreover, the upper edge of the image is located at the same point on the film. The wavelength increases significantly with the heat flux density. In the zone between the falling streamlets the surface of the gas-liquid interface is not smooth. This indicates that the thermocapillary motion is intense.

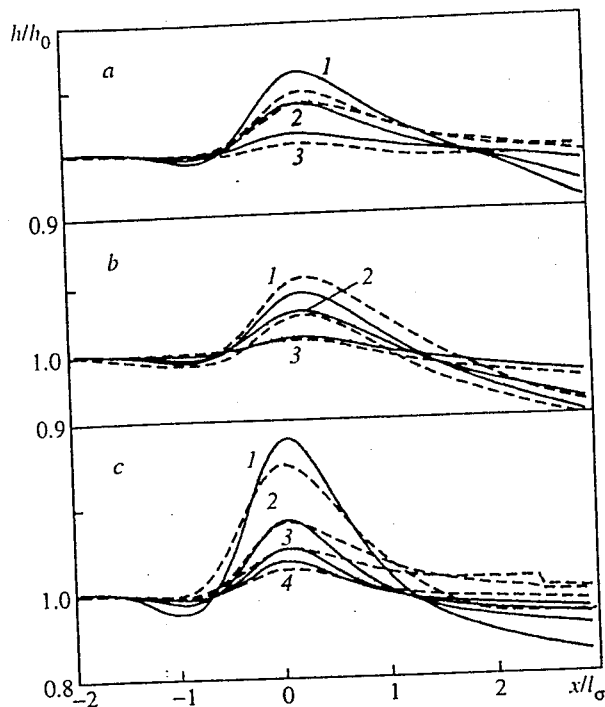


Fig. 5. Relative film thickening as a function of the heat flux density. The broken and continuous curves correspond to experiment and calculation, respectively: (a)  $Re = 2$ ,  $C = 10\%$ , curves 1-3 correspond to  $q = 2.53, 1.49$ , and  $1.35 \text{ W/cm}^2$ , respectively; (b)  $Re = 1$ ,  $C = 25\%$ , curves 1-3 correspond to  $q = 1.87, 1.38$ , and  $0.57 \text{ W/cm}^2$ , respectively; (c)  $Re = 0.5$ ,  $C = 25\%$ , and curves 1-4 correspond to  $q = 1.21, 0.63, 0.41$ , and  $0.3 \text{ W/cm}^2$ , respectively

In order to compare the measured film thicknesses with those calculated on the basis of the above model it is necessary to determine the heat flux distribution  $q(x)$  realized experimentally. The heater surface temperature is not constant due to the increase in the weighted-mean temperature of the liquid as the film flows over the heater. As a result, a heat flux develops from the lower, hotter part of the heater toward the upper part.

The function  $q(x)$  was determined numerically by solving the heat conduction equation for the heating element simultaneously with the heat conduction equation for the traveling nondeformable liquid film. The basic element of the heat source was the cover plate. The condition  $q = \text{const}$  was assumed to be satisfied on the resistor-cover plate boundary. Thermal insulation conditions were imposed on the lateral walls of the cover plate and the film surface.

In Fig. 4 we have plotted the variation of the relative film thickening along the flow ( $Re = 1$ ,  $q = 1.38 \text{ W/cm}^2$ , and  $C = 25\%$ ). The experimental results are compared with the calculations with the influence of the two temperature factors taken separately into account. The calculation which takes only the temperature dependence of the viscosity into account ( $\sigma_T = 0$ ) gives significantly underestimated values of the film thickness (curve 1). The calculation carried out with allowance for only the thermocapillary tangential stress ( $\mu = \mu_0 = \text{const}$ ) gives overestimated values (curve 2). The calculation carried out with allowance for the joint influence of both temperature factors is represented in Fig. 4 by continuous curve 3 and ensures the best agreement with the experimental curve 4. After a certain thickening in the area of the upper heater edge the film thickness may fall to a value smaller than the initial one ( $h/h_0 < 1$ ). Since  $T_x(x, h(x)) \geq 0$  this shape of the curves can be obtained only by taking the temperature dependence of the viscosity into account.

In Fig. 5 we have plotted the variation of the relative film thickening along the plate as a function of the heat flux for various  $Re$  numbers. The results of the calculations with allowance for both temperature factors satisfactorily describe the experimental curves obtained. The measurements and calculations showed that even for small heat fluxes a thermocapillary roller, whose dimensions increase with the heat flux, develops

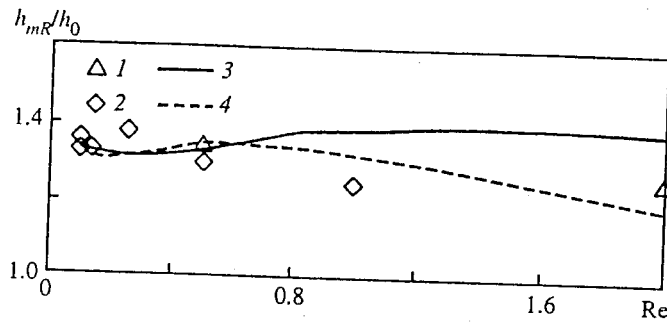


Fig. 6. Maximum film thickness at the instants of regular structure formation and onset of reverse flow: curve 1 corresponds to  $C = 10\%$ , curve 2 to  $C = 25\%$ , curve 3 to  $C = 10\%$ , and curve 4 to  $C = 25\%$

in the zone in which the thermal boundary layer rises to the film surface. The location of the roller vertex, as which we took the point of maximum film thickening, is conserved with respect to the heat flux. With increase in the  $Re$  number the location of the roller vertex is displaced downstream. The distance from a given local minimum of the film thickness to the roller vertex remains almost constant.

In Fig. 6 we have reproduced the results of measuring the critical relative film thickening at the instant of regular structure formation for various  $Re$  numbers and various ethyl alcohol concentrations in the solution. The measurement and calculation results are in satisfactory agreement and indicate that this parameter is only slightly affected by the value of  $Re$ . In the calculations we took the value of  $h_{mR}/h_0$  at the instant of onset of the reverse flow as the critical film thickening. The measurements and calculations give a film thickening of the order of 30% of the initial thickness at the instant of structure formation.

*Summary.* Experiments and numerical calculations carried out with allowance for the temperature dependence of the viscosity and the surface tension show that at small Reynolds numbers in the neighborhood of the upper edge of the heating element there exists a film deformation in the form of a roller even at small heat fluxes. Upstream of the roller, the film is systematically observed to be thinned by 3% of its thickness. Regular structures are formed at a certain almost constant relative roller thickness which is independent of the  $Re$  number of the film. According to the experimental data, this thickness is  $1.32 \pm 0.07$ , which is in satisfactory agreement with the results of the numerical calculations.

The work was carried out with financial support from the complex integration projects Program of the Siberian Branch of RAS, the youth project "Discontinuity of falling films under local heating", and the European Commission under contract ERB IC15-CT98-0908.

## REFERENCES

1. O. A. Kabov, I. V. Marchuk, and V. M. Chupin, "Thermal imaging study of the liquid film flowing on the vertical surface with local heat source," *Russ. J. Eng. Thermophys.*, **6**, No. 2, 104 (1996).
2. O. A. Kabov, "Formation of regular structures in a locally heated falling liquid film," *Teplofizika i Aeromekhanika*, **5**, 597 (1998).
3. O. A. Kabov and I. V. Marchuk, "Regular structures in locally heated falling liquid films," in: *Proc. 2nd Intern. Symp. on Two-Phase Flow Modelling and Experimentation*, Vol. 2, Edizioni ETS, Pisa (1999), P.1225.
4. A. Oron, S. H. Davis, and S. G. Bankoff, "Long-scale evolution of thin liquid films," *Rev. Modern Phys.*, **69**, 931 (1997).
5. S. W. Joo, S. H. Davis, and S. G. Bankoff, "A mechanism for rivulet formation in heated falling films," *J. Fluid Mech.*, **321**, 279 (1996).
6. I. V. Marchuk and O. A. Kabov, "Numerical modelling of thermocapillary reverse flow in thin liquid films under local heating," *Russ. J. Eng. Thermophys.*, **8**, No. 1-4, 17 (1998).
7. G. Gimbutis, *Heat Transfer in Gravitational Liquid Film Flow*, [in Russian], Mokslas, Vil'nyus (1988).